RESEARCH ARTICLE

European Journal of Advanced Chemistry Research
www.ej-social.org

Morphological Behavior of DPPC-DMPC Two-dimensional Mixed Monolayer on Water Surface by Dropping Method

Yuta Watanabe, Daiki Uchida, Honoka Akatsuka, Akihiro Yoshino, Keijiro Taga, Yasushi Yamamoto, Zameer Shervani, and Masato Yamamoto

ABSTRACT

We have investigated the morphology of dipalmitoyl phosphatidyl choline (DPPC)-dimyristoyl PC (DMPC) mixed monolayer formed on the water surface by the dropping method using surface tension measurement (STm), Brewster angle microscopy (BAM), and infrared external reflection spectroscopy (IERS). The limiting molecular area (A_0) obtained by STm showed that the negative deviation at < mole fraction (x_{DMPC})= 0.4 whereas the positive deviation at > x_{DMPC} =0.6 when DMPC was added to the DPPC monolayer. BAM images also showed that the condensed rigid monolayer at x_{DMPC} < 0.4 changed to the expandable monolayer at x_{DMPC} > 0.5. Moreover, IER spectra showed that the alkyl chains of both DPPC and DMPC molecules are in trans conformation in mixed monolayer at x_{DMPC} =0.2 whereas gauche conformation existed at x_{DMPC} = 0.8. Above findings have justified the transition of flexible gauche conformation alkyl chains of DMPC molecule into rigid trans conformation by the addition of DPPC molecule at x_{DMPC} < 0.4 whereas alkyl chains retained flexible gauche conformation in both DPPC and DMPC molecules at x_{DMPC} > 0.6.

Keywords: Dipalmitoyl Phosphatidyl Choline (DPPC); Dimyristoyl Phosphatidyl Choline (DMPC); Mixed Monolayer; Surface Tension Measurement (STm); Brewster Angle Microscopy (BAM); Infrared External Reflection Microscopy (IERS).

Published Online: February 09, 2022

ISSN: 2684-4478

DOI: 10.24018/ejchem.2022.3.1.75

Yuta Watanabe
Department of Life Science and Applied Chemistry, Graduate School of Engineering, Nagoya Institute of Technology, Nagoya, Japan.
Daiki Uchida
Department of Life Science and Applied Chemistry, Graduate School of Engineering, Nagoya Institute of Technology, Nagoya, Japan.
Honoka Akatsuka
Department of Life Science and Applied Chemistry, Graduate School of Engineering, Nagoya Institute of Technology, Nagoya, Japan.
Akihiro Yoshino
Department of Life Science and Applied Chemistry, Graduate School of Engineering, Nagoya Institute of Technology, Nagoya, Japan.
Keijiro Taga
Department of Life Science and Applied Chemistry, Graduate School of Engineering, Nagoya Institute of Technology, Nagoya, Japan.
Yasushi Yamamoto*
Department of Life Science and Applied Chemistry, Graduate School of Engineering, Nagoya Institute of Technology, Nagoya, Japan.
(e-mail: yamamoto.yasushi@nitech.ac.jp)
Zameer Shervani*
Food & Energy Security Research & Product Centre, Sendai, Japan.
(e-mail: shervani.nanotek@gmail.com)
Masato Yamamoto
Department of Chemistry, School of Arts and Sciences, Showa University, Fujiyoshida, Japan.

****Corresponding Author***

I. INTRODUCTION

Biomembrane is an important part of cell organelles enclosing different cell components and performs a number of functions important to keep cell alive and functioning. It separates the intracellular space from outside, maintains a balance between internal and external state of the cell, exchanges information between cells and transports specific functional substances necessary for cell and organelles functioning. The main components of biomembranes are lipids and membrane-protein present in various ratios depending on the type of membrane [1]. 'Fluid mosaic model', proposed by Singer and Nicolson, has

been widely accepted as a basic structure of biomembrane [2]. In this model, functional membrane proteins are buried in lipid-bilayers consisting of various kinds of lipids in the mosaic pattern. Lipids and proteins move freely in bilayer giving fluidic nature to bilayer structure. Phospholipids are main biomembrane's components with glycolipids and cholesterol the other two important molecules involve in signal transduction in *vivo* [1].

The molecular structure of phospholipid molecule comprises of hydrophilic phosphate ester moieties and two alkyl chains as a hydrophobic group. So, phospholipid molecule shows amphiphilic properties and works as a bio-surfactant. In water subphase, stable lipid bilayers structures of vesicles are formed by orienting hydrophilic moieties outside exposing to water and alkyl hydrophobic chains are aggregated inside avoiding water phase. At air/water interface, stable lipid monolayer is formed when hydrophobic alkyl chains are oriented toward the air phase and hydrophilic moieties spread toward the water phase. Because of the unique properties of forming monolayer and bilayer, the phospholipid molecules are widely used to prepare and study the model biomembrane for a number of purposes [3], [4]. Dipalmitoyl phosphatidyl choline (DPPC) and dimyristoyl PC (DMPC) used in this research are typical phospholipids composed of two alkyl chains (C16 for DPPC and C14 for DMPC) and a polar phosphatidyl choline and glycerol-carbonyl moiety as hydrophilic group. The two phospholipids DPPC and DMPC have a slight structural difference. They are widely used to prepare and study the model biomembranes [4]-[6] in the form of gel/liquid-crystal phase transition of bilayers in water and expand/condensation transition of monolayer on the water surface. There is a difference of only two carbon atoms in the alkyl chain between DPPC and DMPC molecules. This small difference greatly affects the properties of the two molecules. For example, gel/liquid-crystal phase transition of DPPC is 41 ºC and that of DMPC is 24 ºC.

In mixed DPPC-DMPC multilamellar phase diagram in water the preferential appearance of gel or liquid crystal phase depends on the mole fractions of each lipid and at specific mole fraction and temperature the two phases coexist [7]-[11]. Apart from multilamellar phase, the DPPC-DMPC two-dimensional mixed monolayer on water surface can be investigated from the viewpoint of observing the changes in monolayer versus mole fractions of the two lipids. The mixed monolayers of other lipids distearoyl phosphatidyl choline (DSPC)-DMPC [12], [13], DSPC-DPPC [14], and DPPC-hexadecanol [15] have been investigated. However, the study of DPPC-DMPC lipid combination is a pending issue. Therefore, in this communication, we have investigated the monolayer properties of two-dimensional DPPC-DMPC mixed monolayer at various mole fractions formed by the dropping method [16], [17], [18], [19] using surface tension measurement (STm), Brewster angle microscopy (BAM), and infrared external reflection spectroscopy (IERS).

II. Experimental

A. Materials

Dipalmitoyl phosphatidyl choline (DPPC, purity: >99%), dimyristoyl phosphatidyl choline (DMPC, purity: >99%), and dimyristoyl-d54 phosphatidyl choline (DMPC (d), purity >99%) were purchased from Avanti polar lipids Inc. (Alabama, USA), respectively, and these were used without further purification. Spreading solvent used for monolayer preparation was chloroform (99.0%, Wako Pure Chemical Industries Ltd.). Purified water with conductance <0.07 μS/cm was obtained using a Super Water Purifying System (WL-21P; Yamato Scientific Corp. Ltd.).

B. Monolayer Formation

Lipids DPPC, DMPC and DMPC(d) were dissolved in chloroform to prepare dropping solutions of 0.5 mM. The dropping solution of pure DPPC, DMPC, DMPC(d) and mixed lipids, depending on the experiment, was dropped on a purified water surface with a 100 μl microsyringe (Ge-0583-04; Hamilton Corp., Nevada, USA) to prepare the monolayer. The experimental details of monolayer formation have been reported previously [16]-[20]. Initially, 1 μl drop of dropping solution was spread gently on the water surface and next drop was added after $\geq$1 min so that previous droplet expanded sufficiently on the water surface. After the addition of each drop of dropping solution containing lipid molecules on the water surface, the attainment of molecular expansion equilibrium was confirmed by surface tension (Section II-III) value till it becomes constant. The completion of monolayer formation was confirmed by the appearance of lens and a constant value of surface tension.

C. Surface Tension Measurement (STm)

Surface tension measurement (STm) for each pure DPPC, DMPC, DMPC (d)) and several mixed monolayers were carried out using a Surface Tensiometer (CBVP-A3; Kyowa Interface Science Corp. Ltd., Saitama, Japan) with a platinum Wilhelmy plate [16]-[20]. Surface tension was recorded after

spreading each drop at 26±1 ºC. The value of surface tension was converted to surface pressure (π). The π -*A* curve of each monolayer was constructed as a function of the dropping volume (molecule numbers).

D. Brewster Angle Microscopy (BAM)

Brewster angle microscopy (BAM) for visualizing the morphology of pure DPPC and DMPC and several mixed monolayers were carried out using a commercial BAM microscope (EMM633K; Filgen Inc., Nagoya, Japan) attached with an USB-CAP type (GV-USB2; I-O DATA DEVICE, INC., Kanazawa, Japan) imaging analysis software [16], [17], [18], [19], [20]. BAM shows the monolayer image arises from the difference in refractive index between the monolayer and the water phase. BAM device was mounted on a glass dish and *p*-polarized light of 632.8 nm wavelength from a 10 mW He-Ne laser was irradiated at the Brewster angle of 53.1° on the surface of pure and mixed monolayers. The reflected light was magnified with a 40 mm focal length lens and detected by a CCD camera (C5948-70; Hamamatsu Photonics, Hamamatsu). The formation of pure and mixed monolayers prepared by dropping method was observed in real-time at 26±1°C. The lateral resolution of BAM image was about 1 μm.

E. Infrared External Reflection Spectroscopy (IERS)

The structure of alkyl chains of DPPC and DMPC molecules in two mixed monolayers consisting of mole fraction of DMPC: 0.2, 0.8 and mole fraction of DMPC(d): 0.2 were studied by infrared external reflection spectroscopy (IERS) [16], [18], [19], [21]. An FT-IR spectrometer (FT-IR-600Plus; JASCO Int. Co. Ltd.) fitted with a liquid-nitrogen-cooled MCT detector and a reflectance apparatus was employed in combination. Dropwise added DPPC-DMPC/chloroform solution was expanded on the water surface in a poly(tetrafluoroethrene) trough (20×62 mm^2) at room temperature, according to the dropping method as described in *Section 2.2*. IERS measurement of mixed monolayer at π=40 mN/m was conducted. *p*-polarized IR light at incident angles of 8-10º and 70-75º was irradiated on each mixed monolayer and reflected light was detected by MCT detector to investigate molecular structure and their orientation. More than 1000 scans were averaged with a resolution of 4 cm^{-1}. The IER spectra were converted to the absorption spectra (*k*-spectra) by the reported method [14] using Lorentz oscillator model (LOM) calculation under the assumptions of the n_∞ values (the real part of complex refractive index) of the limiting of the high-wavenumber are 1.50 and the thickness of each mixed monolayer is 2.3 nm.

III. Results and Discussion

A. π-A Isotherm Curve

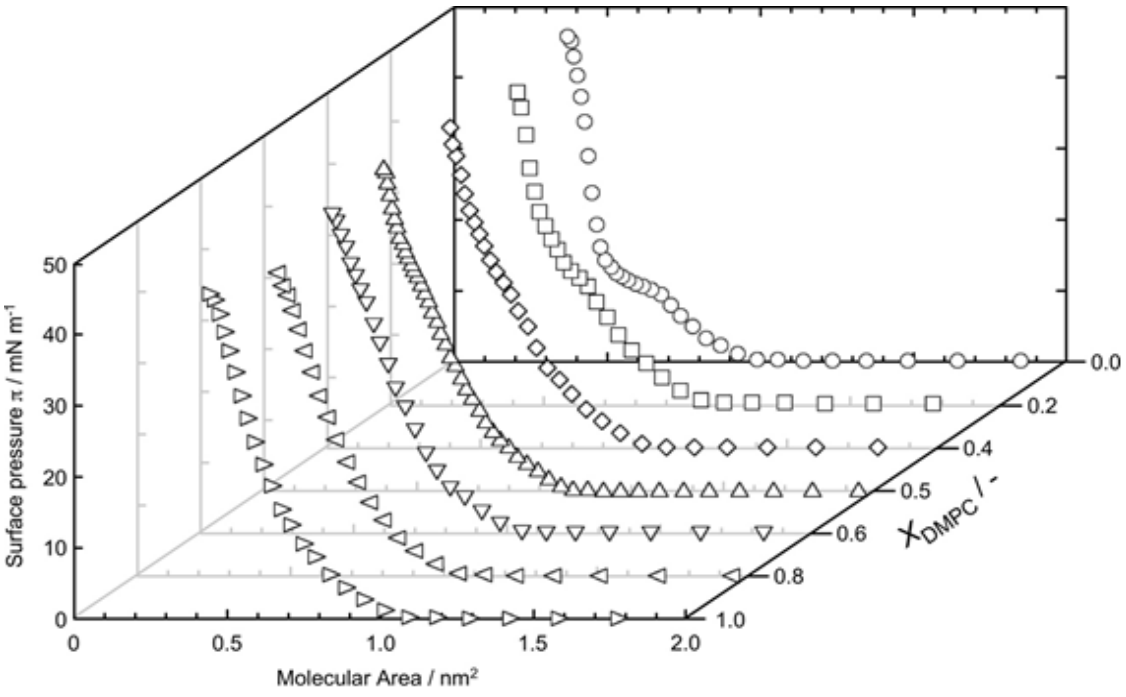

Fig. 1 π-*A* isotherm curves of various DPPC-DMPC mixed monolayers in DMPC mole fraction x_{DMPC} = 0.0, 0.2, 0.4, 0.5, 0.6, 0.8, and 1.0 on the water surface at 26 ˚C using the dropping method.

Fig. 1 shows π versus molecular area *A* (π-*A*) isotherm curves of various DPPC-DMPC mixed monolayers (DMPC mole fraction x_{DMPC} = 0.0, 0.2, 0.4, 0.5, 0.6, 0.8, 1.0) on water surface at 26 ºC constructed by dropping method. Horizontal axis represents *A* calculated from molecular numbers in the

dropping volume, vertical axis is π recorded after dropping the sample solution on the water surface, and depth axis is x_{DMPC}. When π reached at constant value after dropping each droplet, π value was recorded.

At pure DPPC monolayer (x_{DMPC} = 0.0, (○)), π value increased gradually from molecular area > 1.0 nm^2. It was Liquid-Expanded (LE) state till molecular area > 1.0 nm^2. After a transition from LE to Liquid-Condensed (LC) states was observed around 10 mN/m (plateau range), the π increased up to 45 mN/m. The limiting molecular area (A_0) of x_{DMPC} = 0.0 was 0.58 ± 0.02 nm^2/molecule (40 mN/m). This curve was similar to that previously reported [16]-[18], [20]. and also different from that by the compression method [6], [22]. As recorded by compression method [22], the maximum π and A_0 were 50 mN/m and 0.48 nm^2/molecule, respectively. Compared with the compression method, the maximum π was 10% lower and A_0 was 20% larger to the values we recorded by dropping method. A lower π value and larger A_0, suggest the formation of "semi-expanded state" type DPPC monolayer on the water surface which has "fluid structure" where hydrophilic groups (phosphatidyl choline) of DPPC molecules and water molecules are arranged in most comfortably through hydrogen bonding also known as hydrophilic interaction [16].

At the pure DMPC monolayer (x_{DMPC} = 1.0, (▷)), the π -*A* isotherm curve was almost the same as reported previously [17], [23], [24]. π increased gradually from a molecular area > 1.0 nm^2 and kept increasing monotonously up to 45 mN/m. The shape of the curve was smooth and similar to that obtained by compression method [6], [25], [26]. A_0 and π values for x_{DMPC} = 1.0 were 0.75±0.03 nm^2/molecule and 40 mN/m, respectively similar to the values (0.73 nm^2/molecule and 40 mN/m, respectively) obtained by compression method. The recorded A_0 and π values for x_{DMPC} = 1.0 suggested DMPC monolayer is in LE state where two alkyl chains of DMPC molecule were partially disordered. The alkyl chains are in gauche conformation and the cross-sectional area would be larger than that of hydrophilic group of DMPC molecule.

Comparing the pure DPPC monolayer (x_{DMPC} = 0.0, (○)), the shape of π -*A* isotherm curves of DPPC-DMPC mixed monolayer changed gradually with the increase in mole fraction of DMPC (from 0.2 to 0.8) as following. At x_{DMPC} = 0.2 (□), the π increased gradually from a molecular area > 1.0 nm^2 similar to x_{DMPC} = 0.0. Though, the plateau region observed at x_{DMPC} = 0.0 did not exist. Instead, the curve bent at 15 mN/m and after that increased linearly. From 22 mN/m onward the π increased to 44 mN/m. A_0 of x_{DMPC} = 0.2 was 0.57 ± 0.01 nm^2/molecule at 40 mN/m which was almost the same as of DPPC monolayer. At x_{DMPC} = 0.4 (◇), the curve was little different from that of x_{DMPC} = 0.2. and 0.0. π increased gradually from a molecular area > 1.0 nm^2 same as for x_{DMPC} = 0.2 and 0.0. The bending of the curve was observed at 16 mN/m and then increased linearly. The slope of the linear increase for x_{DMPC} = 0.4 was larger than for x_{DMPC} = 0.2. π increased steeply from 32 mN/m to 45 mN/m. A_0 of x_{DMPC} = 0.4 was 0.64±0.02 nm^2/molecule at 40 mN/m and the value of A_0 was larger than those of x_{DMPC} = 0.0 and 0.2. At x_{DMPC} = 0.5 (△), the curve was close to that of x_{DMPC} = 0.4 and A_0 was also the same as that of x_{DMPC} = 0.4 (0.66 ± 0.02 nm^2/molecule (40 mN/m)). At x_{DMPC} = 0.6 (▽), the curve was a little different from those of $<x_{DMPC}$ = 0.5. π increased gradually from molecular area > 1.0 nm^2 and the curve bent at 34 mN/m. After that π increased steeply from 38 to 45 mN/m. A_0 for x_{DMPC} = 0.6 was 0.76 ± 0.02 nm^2/molecule at 40 mN/m which was close to the DMPC monolayer. At x_{DMPC} = 0.8 (◁), the curve was different from those of $<x_{DMPC}$ = 0.6 and very similar to x_{DMPC} = 1.0. π increased gradually from a molecular area > 1.0 nm^2 and further increased monotonously up to 43 mN/m. The shape of curve was as smooth as that of x_{DMPC} = 1.0. A_0 for x_{DMPC} = 0.8 was also 0.77 ± 0.02 nm^2/molecule at 40 mN/m and it was close to that of DMPC monolayer. These results suggested that the formation of DPPC-DMPC mixed monolayer was very different for each mole fraction (x_{DMPC}) of DMPC.

B. Brewster Angle Microscopy (BAM)

Fig. 2 shows a series of BAM images of DPPC-DMPC mixed monolayers in DMPC mole fraction ratios x_{DMPC} = 0.0, 0.2, 0.4, 0.5, 0.6, 1.0 on the water surface at 26 ºC. Fig. 2a-c, 2d-f, 2g-I, 2j-l, 2m-o, and 2p-r are DPPC-DMPC mixed monolayer of x_{DMPC} = 0.0, 0.2, 0.4, 0.5, 0.6, and 1.0 respectively. BAM observation was performed on each monolayer at the dropping volume corresponding to three π values as shown in the inset of the figures.

At the DPPC monolayer of x_{DMPC} = 0.0 (Fig. 2a-c), images resembled with those previously reported [16]-[18]. Image 2a at π = 4.1 mN/m is of the monolayer before LE-LC transition and showed a homogeneous dark contrast. Image 2b of π = 10.5 mN/m around LE-LC transition is the monolayer where phases (LE and LC phase) coexist and showed hole-type dark parts in bright domain (spot-type pattern). This pattern was different from that by the compression method [27]. Image 2c of π = 42.3 mN/m is the monolayer after LE-LC transition and showed a homogeneous bright contrast. These images indicate that fluidic DPPC monolayer in "semi-expanded state" type domain was formed on the water surface by the dropping method. This result also corresponded to that obtained by the π -*A* isotherm curve (Fig. 1 (○)).

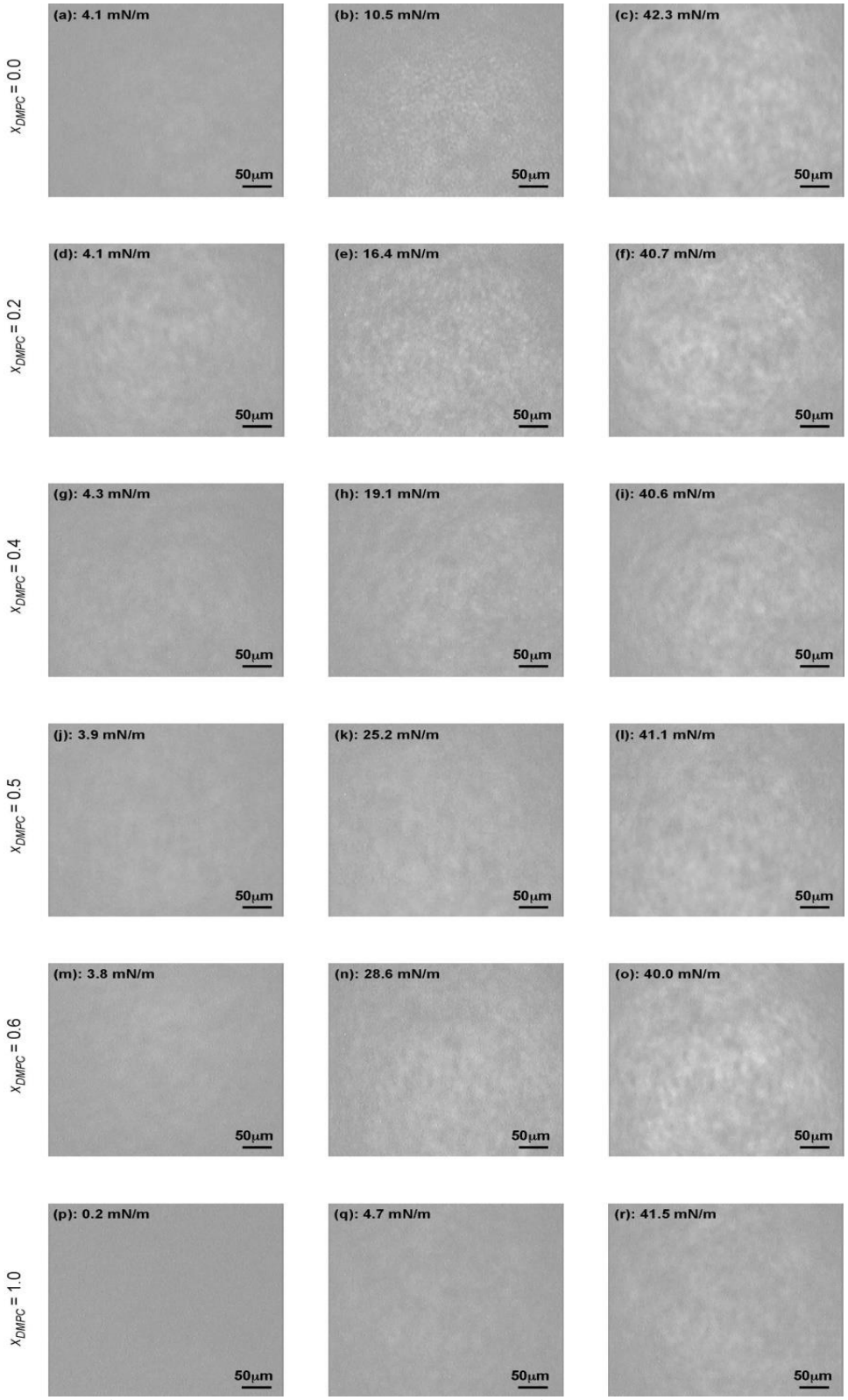

Fig. 2. BAM images of various DPPC-DMPC mixed monolayers (DMPC mole fraction x_{DMPC} = 0.0, 0.2, 0.4, 0.5, 0.6, and 1.0) on the water surface at 26 ˚C. x_{DMPC} of (a-c) 0.0 (pure DPPC monolayer); (d-f) 0.2; (g-i) 0.4; (j-l) 0.5; (m-o) 0.6; and (p-r) 1.0 (pure DMPC monolayer).

At the DMPC monolayer of x_{DMPC} = 1.0 (Fig. 2p-r), images resembled with those previously reported [17], [24]. Image 2p of π = 0.2 mN/m showed a homogeneous dark contrast. With increasing in π, the image became bright. Image 2q of π = 4.7 mN/m was brighter than image 2p of π = 0.2 mN/m, indicated that DMPC monolayer continued to form homogeneously. Image 2r of π = 41.5 mN/m showed still brighter homogeneous contrast. The pattern of these three images indicated that expandable DMPC monolayer was formed on the water surface by the dropping method. The result also corresponded to that obtained by π -*A* isotherm curve (Fig. 1 (▷)) and was the same as reported previously by the compression

method [28].

BAM images of DPPC-DMPC mixed monolayer changed gradually according to an increase in the mole fraction of DMPC (from 0.2 to 0.8) as following. At x_{DMPC} = 0.2 (Fig. 2d-f), the images resembled with those of pure DPPC monolayer. Image 2d of π = 4.1 mN/m showed a homogeneous dark contrast. Image 2e of π = 16.4 mN/m showed a coexistence state that has hole-type dark parts bright domain (spot-type pattern). The image resembled with image 2b of pure DPPC monolayer. From the image, it was found that the slope of the isotherm curve from 15 to 22 mN/m in Fig. 1(□) indicated LE-LC transition of mixed monolayer at x_{DMPC} = 0.2. Image 2f of π = 40.7 mN/m showed a homogeneous bright contrast. At x_{DMPC} = 0.4 (Fig. 2g-i), the images were a little different from those of x_{DMPC} = 0.2. Image 2g of π = 4.3 mN/m showed a homogeneous dark contrast. Image 2h of π = 19.1 mN/m showed brighter image than that of π = 4.3 mN/m (image 2g). The image also showed slightly spot-type pattern as observed at image 2e of x_{DMPC} = 0.2, but it was less clear. Image 2i showed a homogeneous bright contrast. At x_{DMPC} = 0.5 (Fig. 2j-l), images were different from those of x_{DMPC} = 0.2 and 0.4. Image 2j of π = 3.9 mN/m showed a homogeneous dark contrast. Image 2k of π = 25.2 mN/m showed brighter image than that of π = 3.9 mN/m (image 2j). The image did not show spot-type pattern as observed at image 2e of x_{DMPC} = 0.2. Image 2l showed a homogeneous bright contrast. These images resembled with those of pure DMPC monolayer. At x_{DMPC} = 0.6 (Fig. 2m-o), the images resembled with those of pure DMPC monolayer (2p-r) and similar to those of x_{DMPC} = 0.5. Image 2m of π = 3.8 mN/m showed a homogeneous dark contrast. Image 2n of π = 28.6 mN/m showed brighter image than that of π = 3.8 mN/m (image 2m). Image 2o of π = 40.0 mN/m showed a homogeneous bright contrast. The results of BAM observation suggested that the formation process of DPPC-DMPC mixed monolayer changed with an increase in mole fraction of DMPC.

C. Compression Moduli

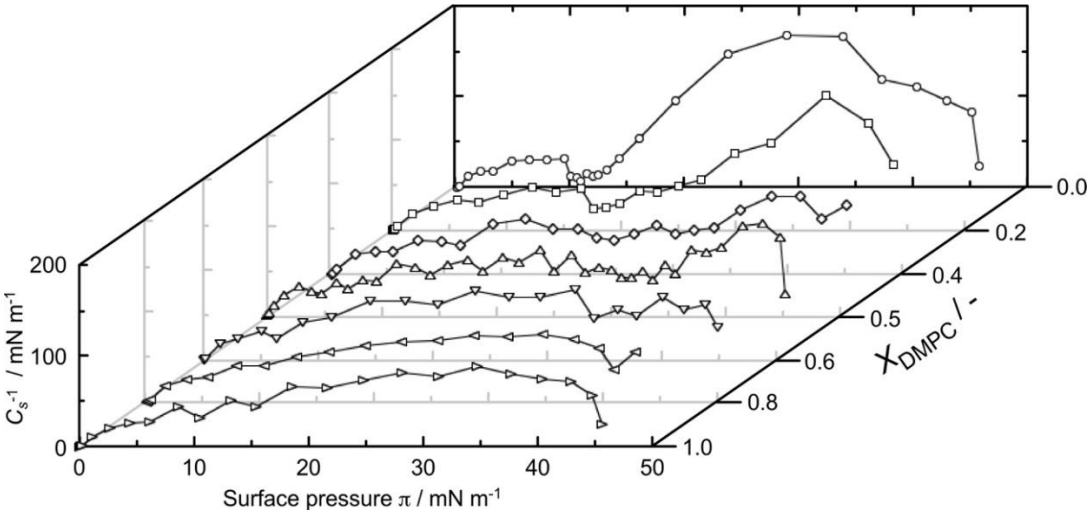

Fig. 3 C_s^{-1}-π profiles of various DPPC-DMPC mixed monolayers (DMPC mole fraction x_{DMPC} = 0.0, 0.2, 0.4, 0.5, 0.6, 0.8, and 1.0) calculated from the π -*A* isotherm curves in Fig. 1.

In order to obtain more detailed information from the obtained π -*A* isotherm curves (Fig. 1) and BAM observations (Fig. 2), the compression moduli (C_s^{-1}) have been calculated for each *π-A* isotherm curves (Fig. 1). C_s^{-1} is described by the following formula,

$$C_s^{-1} = -A(d\pi/dA)$$

where *A* is the molecular area(nm^2/molecule), π is the surface pressure (mN/m). The values of compression moduli are used conventionally as a tool for considering the physicochemical state of a Langmuir monolayer [29]-[32]. The monolayer state is distinguished in following states; gaseous (G), liquid expanded (LE), liquid condensed (LC), and solid (S). The values of C_s^{-1}: <12, 12 -100, 100 -250, and > 250 mN/m corresponded to G, LE, LC, and S state.

Fig. 3 shows C_s^{-1} versus π profiles of various DPPC-DMPC mixed monolayers of x_{DMPC} = 0.0, 0.2, 0.4, 0.5, 0.6, 0.8, and 1.0 on the water surface at 26 ºC. Horizontal axis represents π, vertical axis represents calculated C_s^{-1} parameter values, and depth axis is x_{DMPC}. At the pure DPPC monolayer (x_{DMPC} = 0.0, (○)), there were two processes. At first process, the C_s^{-1} value increased gradually until around 10 mN/m. The maximum C_s^{-1} value was 25 mN/m and referred to LE state. At second process after showing a steep dip corresponding to LE-LC transition (10 mN/m), the C_s^{-1} value increased again until 34 mN/m. The rate of

the increase was larger than that of first process. Maximal C_s^{-1} value was 170 mN/m and referred to LC state. With decrease in the value more than 34 mN/m, monolayer formation was completed. This profile is a characteristic of a monolayer causing two-dimensional phase transition (LE-LC transition). The maximum C_s^{-1} value (170 mN/m) of second process was smaller than the value (220 mN/m) obtained by the compression method [22], [33]. This indicates that the DPPC monolayer formed by the dropping method is "semi-expanded state" type monolayer as mentioned in the section 3.1 (π -*A* isotherm).

At the pure DMPC monolayer (x_{DMPC} = 1.0, (▷)), there was one process different from that of DPPC monolayer (○). The C_s^{-1} value increased gradually and monotonically until 35 mN/m. With decrease in the value more than 35 mN/m, monolayer formation was completed. The maximum C_s^{-1} value was ca. 90 mN.m and referred to LE state. This profile is a characteristic of a LE monolayer, different from that of pure DPPC monolayer. The maximal C_s^{-1} value (90 mN/m) was a little smaller than the value (100 mN/m) obtained by the compression method [33]. This indicates that the DMPC monolayer by the dropping method is certainly LE type as mentioned in section 3.1 (π -*A* isotherm).

The shape of C_s^{-1}- π profiles of DPPC-DMPC mixed monolayer changed gradually according to an increase in the mole fraction of DMPC from 0.2 to 0.8 as following. At x_{DMPC} = 0.2 (□), there were two processes similar to that of pure DPPC monolayer of x_{DMPC} = 0.0. At the first process, the C_s^{-1} value increased gradually until 17 mN/m and reached a maximal value of 50 mN/m and referred to LE state. This process overlapped and became extension of DPPC monolayer. This indicated that the tendency of LE state is stronger than that of pure DPPC monolayer. At the second process where a steep dip corresponding to LE-LC transition of mixed monolayer was noticed, the value increased again until 39 mN/m. The rate of the increase after the dip was similar to that of DPPC monolayer. The maximal value reached to 150 mN/m and referred to LC state. This value remained lower than that of pure DPPC monolayer of the second increased process. With decrease in the value more than 39 mN/m, monolayer formation was completed. This result was a little different from that of pure DPPC monolayer. This indicates that the rigidly of DPPC-DMPC mixed monolayer of x_{DMPC} = 0.2 was reduced by mixing LE-type DMPC molecules. In other words, increase in elasticity was noticed compared to pure DPPC monolayer. At x_{DMPC} = 0.4 (◇), there were two processes different from those of less than x_{DMPC} = 0.2. At first process, the C_s^{-1} value increased gradually until 17 mN/m. The maximum value was 50 mN/m and referred to LE state. This process is similar to those of less than x_{DMPC} = 0.2. At the second process noticed at 17 mN/m, on the other hand, the C_s^{-1} decreased and increased gently until 33 mN/m, and subsequent increased faster until 40 mN/m. The gentle decrease process was different from the steep dip at less than x_{DMPC} = 0.2. The LE-LC transition observed at less than x_{DMPC} = 0.2, has not occurred. With decrease in the value more than 40 mN/m, monolayer formation was completed. The maximum C_s^{-1} value of the second process was 90 mN/m and referred to LE state. This indicates that the mixed monolayer of x_{DMPC} = 0.4 changed from elastic state of x_{DMPC} = 0.2 into semi-expand state. At x_{DMPC} = 0.5 (△), there were two processes similar to x_{DMPC} = 0.4. At first process, the C_s^{-1} value increased gradually until around 25 mN/m. The maximum value was 60 mN/m and referred LE state. At the second process more than 25 mN/m, the C_s^{-1} decreased and increased gently until 36 mN/m, and subsequent increased faster until 42 mN/m. With decrease in the value more than 42 mN/m, monolayer formation was completed. The maximum C_s^{-1} value of the second process was 100 mN/m and referred to LE state. This process was similar and a slight shift to the right compared to that of x_{DMPC} = 0.4. This indicates that the mixed monolayer of semi-expand state was promoted at x_{DMPC} = 0.5 compared to the state of x_{DMPC} = 0.4. At x_{DMPC} = 0.6 (▽), there was a different process compared to those of x_{DMPC} = 0.4 and 0.5. At less than 32 mN/m, C_s^{-1} value increased gradually resembled to those of x_{DMPC} = 0.2, 0.4, and 0.5. The maximum value was 80 mN/m and referred to LE state. After showing the steep dip and the minimum C_s^{-1} value of 50 mN/m at 33 mN/m, the value increased gently and the monolayer formation was completed with decrease in the value at 45 mN/m. The slop of the increase was similar to that of gentle increase in the second process of x_{DMPC} = 0.2 and 0.4. This indicates that the mixed monolayer of x_{DMPC} = 0.6 changed from semi-expand state of x_{DMPC} = 0.5 into expand state. At x_{DMPC} = 0.8 (◁), there was one process similar to that of x_{DMPC} = 1.0. The C_s^{-1} value increased gradually and monotonously until 35 mN/m. With decrease in the value more than 35 mN/m, monolayer formation was completed. The maximum C_s^{-1} value was 75 mN/m and referred to LE state. This indicates that the mixed monolayer of x_{DMPC} = 0.8 is certainly in an expand state, in other words, LE monolayer. These results of C_s^{-1} parameters suggest that an increase in x_{DMPC} changes dynamically the state of DPPC-DMPC mixed monolayer.

D. Mole Fraction of DMPC (x_{DMPC}) Dependence of A_0

A_0s of DPPC-DMPC mixed monolayers were compared to those of ideal mixed monolayers calculated from each A_0 of DPPC and DMPC monolayers. Fig. 4a (○) shows x_{DMPC} dependence of A_0 derived from π-*A* isotherm curves in Fig. 1. The horizontal axis represents x_{DMPC} and the vertical axis represents A_0 of

each x_{DMPC}. The x_{DMPC} = 0.0 and 1.0 are pure DPPC and DMPC monolayers, respectively. The dotted line is drawn as an ideal additivity to each x_{DMPC}.

At x_{DMPC} = 0.2, the value of A_0 was almost the same as that of x_{DMPC} = 0.0 similar pattern noticed in π - *A* Isotherm (section 3.1) and also showed a negative deviation from the ideal value. This indicates that the flexible alkyl chain of DMPC molecule at x_{DMPC} = 0.2 was affected by the rigid alkyl chain of DPPC molecule. At x_{DMPC} = 0.4 and 0.5, the values of A_0s were overlapped with the ideal (dotted) line. In these mole fractions DPPC and DMPC molecules mixed ideally. Therefore, both molecules existed in a state where they do not interact with each other in the mixed monolayer. At x_{DMPC} = 0.6 and 0.8, on the other hand, the values of A_0s were almost the same as that of monolayer of x_{DMPC} = 1.0 similar to noticed in the π-*A* isotherm curve (Section III, A) and also showed a positive deviation from the ideal value. This indicates that the rigid alkyl chain of DPPC molecule at x_{DMPC} = 0.6 and 0.8 was affected by the flexible alkyl chain of DMPC molecule on the contrary to the case of x_{DMPC} = 0.2.

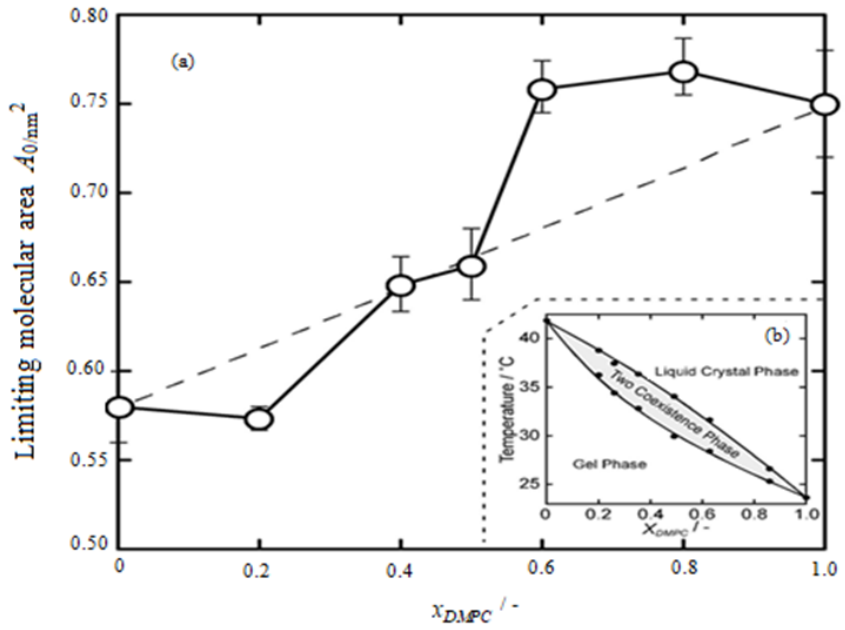

Fig. 4 (a) x_{DMPC} dependence of A_0 derived from the π -*A* isotherm curves in Fig. 1. The dotted line is drawn as an ideal additivity on each x_{DMPC} (b) phase diagram at various mixing ratio of DPPC and DMPC bulk phase (multilamellar vesicle in water).

The above dependence of A_0s on x_{DMPC} was specific to the DPPC-DMPC mixed monolayer and different from that of other mixed monolayers such as DPPC-Chol (Chol: cholesterol) and DMPC-Chol monolayers which had a negative deviation from the ideal value appeared due to the condensation effect of Chol as reported in the earlier studies [18], [22], [24], [26], [34], [35]. The results obtained from A_0 versus x_{DMPC} plot of DPPC-DMPC monolayer will help to understand the macroscopic phase diagram of DPPC-DMPC mixture. Fig. 4b inserted in Fig. 4a shows a phase diagram prepared from observations of mixing DPPC and DMPC in different ratios forming multilamellar vesicle in water. The phase diagram was constructed from the transition curves observed by differential scanning calorimetry (DSC) [7], [8]. The horizontal axis represents x_{DMPC} and the vertical axis represents the phase transition temperature at various x_{DMPC}. On the temperature range 24 to 41 ºC, DPPC-DMPC mixture (vesicle) is transferred from the gel phase to the liquid-crystal phase via the two-phase coexistence region with an increase in x_{DMPC}. It is well known that alkyl chains in vesicle are in a state close to crystal state (all-trans type) in the gel phase, a state close to liquid (gauche type) in the liquid-crystal phase, a mixed state including both gel and liquid-crystal phases exists in coexistence region [1], [4], [7]-[11]. The 3-dimensional macroscopic phase diagram is not always enough to explain 2-dimensional monolayer state. The specific x_{DMPC} dependence of A_0 observed in mixed monolayer is related to the macroscopic phase diagram. Therefore, the mixed monolayer of less than x_{DMPC} = 0.2 corresponds to a gel-type state. Those at x_{DMPC} = 0.4 and 0.5 fit to the ideal (dotted) line in the Fig. 4a corresponds to a two-phase coexistence state. That at more than = 0.6 corresponds to a liquid-crystal type state. Based on the above description, the temperature (26.0 ºC) of the state transfer at the mixed monolayer was lower than that shown in the macroscopic phase diagram (33 ºC) in Fig. 4b. As for this difference, Kajiyama *et al*. [36] have reported that the melting point of two-dimensional crystalline monolayer of several fatty acids was lower than that of their three-dimensional bulk crystalline states. Therefore, the above temperature difference appears as a difference in dimension.

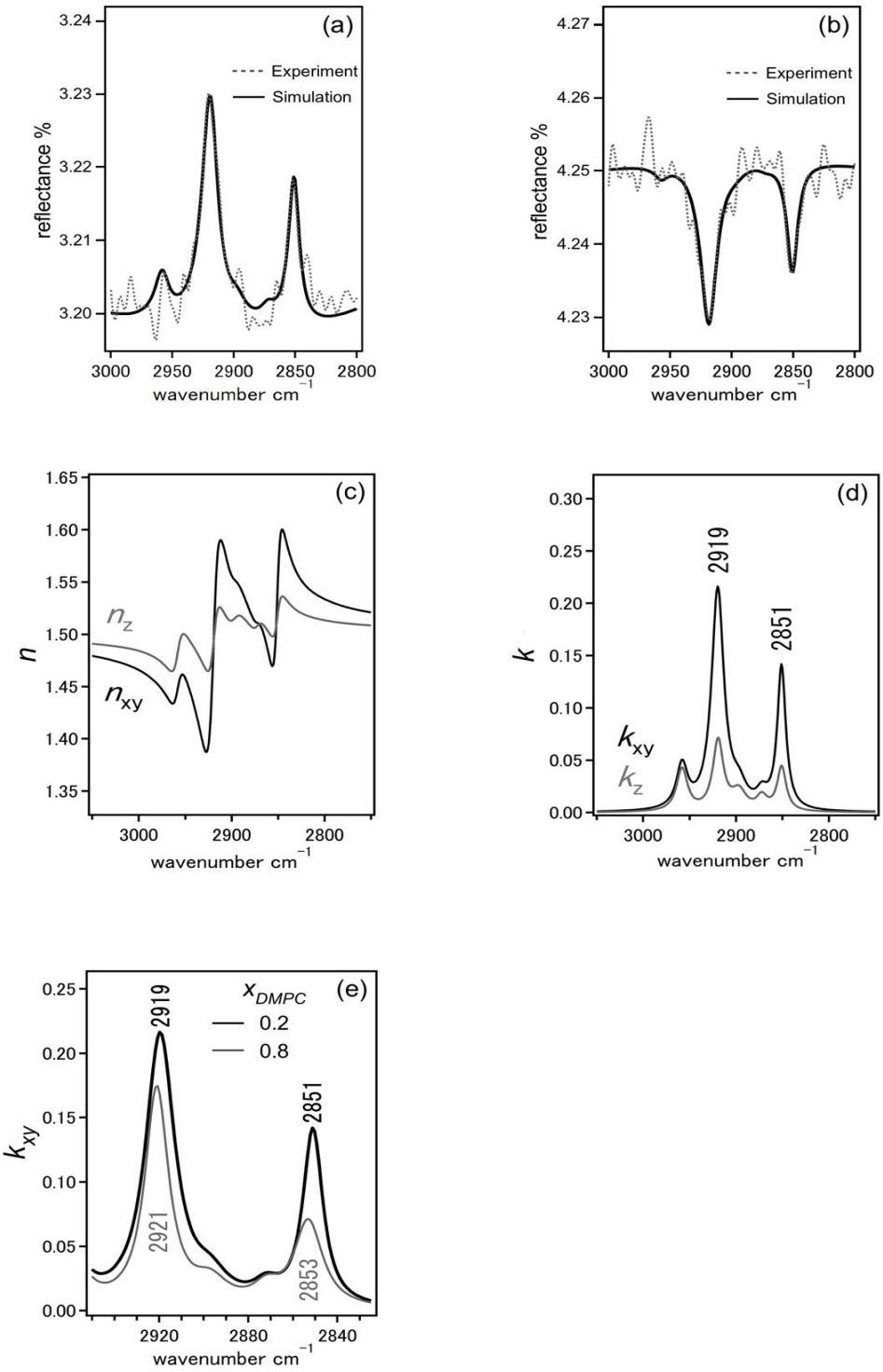

Fig. 5(a-e) IER spectra of DPPC-DMPC mixed monolayer of x_{DMPC} = 0.2 and 0.8 at around a pressure of 38 mN/m in Fig. 1; incident angle is 8˚ (a) and 70˚(b); dotted-line is measured spectrum and solid-line is the simulated spectrum; for x_{DMPC} = 0.2. (c, d): wavenumber dependence of complex refractive index ($n + k_i$), n-spectrum of real part (c) and *k*-spectrum of imaginary part (d), for x_{DMPC} = 0.2. (d) is also absorption spectra (*k*-spectra); (e) kxy-spectra of x_{DMPC} = 0.2 (black line) and x_{DMPC} = 0.8 (gray line) for comparison.

E. Infrared External Reflection Spectroscopy (IERS)

To investigate the molecular-level state based on the specific x_{DMPC} dependence of A_0 in Fig. 4a, we have performed the IERS measurement of DPPC-DMPC mixed monolayers in two mole fraction ratios of x_{DMPC} = 0.2 and 0.8, to study the alkyl chain conformation structure of DPPC and DMPC molecules. Fig. 5a and b show IER spectra of DPPC-DMPC mixed monolayer of x_{DMPC} = 0.2 at a pressure of 38 mN/m, measured at an incident angle of 8º (Fig. 5a) and 70º (Fig. 5b). The horizontal axis represents wavenumber (cm^{-1}) and the vertical axis is reflectance (%). In both Fig. 5a and b, dotted-line shows measured spectrum and solid-line is simulated spectrum. More, their two lines are offset to overlay the

experimental and simulated values. Fig. 5c and d show wavenumber dependence of complex refractive index ($n + k_i$) of the mixed monolayer obtained from the above simulated calculation. Fig. 5c is n-spectrum of real part and Fig. 5d is k-spectrum of imaginary part. Moreover, Fig. 5d corresponds to the absorption spectra (*k*-spectra). The horizontal axis represents wavenumber (cm^{-1}) and the vertical axis represents intensity of each real and imaginary part, indicating the components of parallel to the surface plane (in plane) by black lines (n_{xy}, k_{xy}) and the components perpendicular to the surface plane (out of plane) by gray lines (n_z, k_z) (Yamamoto et al. 2008). Fig. 5e shows the absorption spectra (k_{xy}-spectra) of x_{DMPC} = 0.2 (black line) and x_{DMPC} = 0.8 (gray line). The same analysis of x_{DMPC} = 0.2 has been also performed about x_{DMPC} = 0.8. On Fig. 5e, the horizontal axis represents wavenumber (cm^{-1}) and the vertical axis represents the absorption spectra of each k_{xy} (in plane) of x_{DMPC} = 0.2 and 0.8. After that, we will discuss k_{xy} spectra that appeared clearly by the IERS measurement for comparison of x_{DMPC} = 0.2 and 0.8.

On the k_{xy}-spectra (Fig. 5e) at x_{DMPC} = 0.2 (black line), two absorption peaks at 2919 cm^{-1} and 2851 cm^{-1} were selected for simulation. These peaks were assigned to CH_2 anti-symmetric stretching vibration band $\nu_{as}(CH_2)$ and CH_2 symmetric stretching vibration band $\nu_s(CH_2)$, respectively. Two peaks at 2919 cm^{-1} and 2851 cm^{-1} were strong in particular. These two peaks were of the methylene groups in the two long alkyl chains of DPPC and DMPC molecules. As reported previously [21], [37], it is known that when the alkyl chain has a structure which contains trans conformation to a certain degree in the chain, two $\nu_{as}(CH_2)$ and $\nu_s(CH_2)$ bands of methylene group in the chain are assigned to 2919 cm^{-1} and 2851 cm^{-1} bands, respectively. In the case of pure DPPC monolayer at 26 ˚C, we reported that two peak positions of those $\nu_{as}(CH_2)$ and $\nu_s(CH_2)$ bands at π = 42 mN/m were shown at 2919 cm^{-1} and 2851 cm^{-1} and those alkyl chains stood toward to normal of monolayer surface [16]. In the case of pure DMPC monolayer at 26 ºC, on the other hand,two $\nu_{as}(CH_2)$ and $\nu_s(CH_2)$ bands of methylene group of alkyl chain of DMPC molecule are assigned to 2920 cm^{-1} and 2852 cm^{-1} bands, respectively, and contains kinked form (gauche conformation) in the chain [24]. It is suggested that the form of the two alkyl chains in the DPPC and DMPC molecules in the mixed monolayer are straightened regularly. Therefore, the result indicates that the kinked form of alkyl chain of DMPC molecule decreased and the structural transition from gauche- to trans- conformation was caused by the presence of DPPC molecule. In other words, DMPC molecules of x_{DMPC} = 0.2 had a stable and condensed structure like pure DPPC molecules, which did not disturb the mixed monolayer structure. These results correspond to the value of A_0 of x_{DMPC} = 0.2 in Fig. 4a was almost the same as that of x_{DMPC} = 0.0.

On the k_{xy}-spectra (Fig. 5e) at x_{DMPC} = 0.8 (gray line), two absorption peaks at 2921 cm^{-1} ($\nu_{as}(CH_2)$) and 2853 cm^{-1} ($\nu_s(CH_2)$) were selected for the simulation. These peaks were also assigned to $\nu_{as}(CH_2)$ and $\nu_s(CH_2)$, respectively, as same as those of x_{DMPC} = 0.2. These two peaks were mainly due to the methylene groups in the two long alkyl chains in the DPPC and DMPC molecules. These peaks showed more high wavenumber on both $\nu_{as}(CH_2)$ and $\nu_s(CH_2)$ bands (2921 cm^{-1} and 2853 cm^{-1}), compared to previous reported peak positions (2920 cm^{-1} and 2852 cm^{-1}). Therefore, the result indicates that DPPC-DMPC mixed monolayer at x_{DMPC} = 0.8 contains irregular structure (gauche conformation) to a large degree in both DMPC and DPPC alkyl chains. In other words, it means that two alkyl chains in DPPC molecules at x_{DMPC} = 0.8 are also the structure containing gauche conformation. These results correspond to that the value of A_0 of x_{DMPC} = 0.8 in Fig. 4a was almost the same as that of x_{DMPC} = 1.0.

In order to elucidate the details of the structural difference between DPPC and DMPC molecules in mixed monolayer at x_{DMPC} = 0.2, we have performed IERS measurement using a dimyristoyl-d54 phosphatidyl choline (DMPC(d)) molecule in which hydrogen atoms of two alkyl chains are deuterated. Fig. 6 shows IER spectra (*k*-spectra) of DPPC-DMPC(d) mixed monolayer of mole fraction of DMPC(d) ($x_{DMPC(d)}$) = 0.2 at a pressure of 38 mN/m, which were simulated from the two reflectance spectra measured at an incident angle of 8º and 70º. The horizontal axis represents wavenumber (cm^{-1}) and the vertical axis represents the intensity of absorption spectra of each k_{xy} and k_z. The method of analysis is as same as mixed monolayers of x_{DMPC} = 0.2 and 0.8. For comparison, we also added *k*-spectra of x_{DMPC} = 0.2 (Fig. 5d) in Fig. 6. k_{xy} spectra at $x_{DMPC(d)}$ = 0.2 is shown as continuous black line that of x_{DMPC} = 0.2 as dotted black line. Similarly, k_z spectra at $x_{DMPC(d)}$ = 0.2 is shown as continuous gray continuous line, that of x_{DMPC} = 0.2 as dotted gray line. In addition, we have confirmed that π -*A* isotherm curve of $x_{DMPC(d)}$ = 0.2 was the same as that of x_{DMPC} = 0.2.

On the spectra in Fig. 6, two strong absorption peaks were observed at around 2918 cm^{-1} and 2850 cm^{-1}. These peaks were assigned to CH_2 anti-symmetric stretching vibration band $\nu_{as}(CH_2)$ and CH_2 symmetric stretching vibration band $\nu_s(CH_2)$, respectively. These two peaks were due to the methylene groups in the two long alkyl chains of only DPPC molecules because peaks of DMPC(d) were another wavenumber region around 2150 cm^{-1} [38], [39]. Actually, the peak intensity of two CH_2 stretching vibration bands certainly decreased as shown by two downward arrows (black and gray). We focused the above two arrows. The decrease in peak intensity of $\nu_s(CH_2)$ around 2850 cm^{-1} was observed only in the k_{xy} spectra

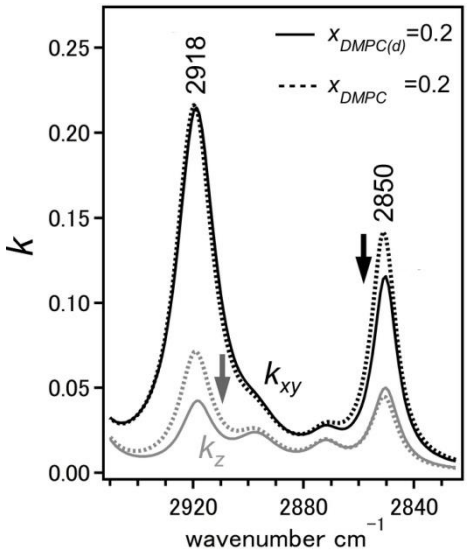

Fig. 6. k-spectra of DPPC-DMPC(d) mixed monolayer of $x_{DMPC(d)}$ = 0.2 at around a pressure of 38 mN/m (continuous line), containing k-spectra of x_{DMPC} = 0.2 in Fig. 5d (dotted line) for comparison.

of black line and not in that of gray line. The decrease in peak intensity of $\nu_{as}(CH_2)$ at around 2918 cm^{-1}, on the other hand, was observed only in the k_z spectra of gray line and not in that of black line. Yamamoto *et al.* have reported using infrared reflection absorption spectroscopy (IRAS) [40] . that the molecular orientation of *n*-alkane tetratetracontane (TTC, *n*-$C_{44}H_{90}$) vacuum-deposited on the Au substrate showed "flat-on" structure of *all*-trans conformation (molecular skeleton plane) in first TTC layer on Au surface. Applying this analytical method, our results indicate that two alkyl chains in DMPC molecule that occupy 20 % (x_{DMPC} = 0.2) in DPPC-DMPC mixed monolayer orient parallel to the water surface and molecular skeleton planes are also parallel to the surface (flat-on orientation). The orientation of DMPC molecules in the mixed monolayer is in contrast to that of DPPC molecules whose alkyl chains are nearly perpendicular to the surface. This indicates that the mixed monolayer mainly composed of DPPC molecules (x_{DMPC} = 0.2) has a structure that can contain 20 % DMPC molecules in the monolayer while maintaining its stable structure, despite the difference in the orientation between DPPC and DMPC molecules.

IV. Conclusion

In this research, we have investigated the morphology of DPPC-DMPC mixed monolayer formed by the dropping method. The π -*A* isotherm curves by STm on various DPPC-DMPC mixed monolayer showed that the addition of DMPC to the DPPC monolayer at less than $x_{DMPC} < 0.4$ retained condensed state like pure DPPC monolayer whereas expandable state like pure DMPC monolayer existed at more than $x_{DMPC} > 0.6$. The BAM observation also supported STm results; the images at $x_{DMPC} < 0.4$ brightened gradually with increase in dropping volume, followed by bright and dark contrast and finally brightening of image noticed. At $x_{DMPC} > 0.5$, the image gradually became brighter until the completion of monolayer. Moreover, IER spectra showed the structural transition (gauche- to trans-conformation) of alkyl chains in DMPC molecule by the rigid structured DPPC molecule at x_{DMPC} = 0.2, and the structural retention (gauche conformation) of alkyl chains in both DPPC and DMPC molecules at x_{DMPC} = 0.8 was found. These results indicate that the three-dimensional bulk structural properties of DPPC-DMPC mixture are also reflected at the two-dimensional DPPC-DMPC mixed monolayer level on the water surface.

References

[1] Shimabayashi S, Terada H, Okabayashi H. *Biocolloid 1&2*. Hirokawa Publishing, Tokyo; 1990.
[2] Singer SJ, Nicolson GL. The Fluid Mosaic Model of the Structure of Cell Membranes, *Science*. 1972;175:720-731.
[3] Gennis RG. *Biomembrane, molecular structure and function.* SPRINGER, New York. 1990.
[4] Hatta I, Murata M. *Dynamics of Biomembrane*. Kyoritsu Shuppan Co., Ltd., Tokyo; 2000.
[5] Matsuki H, Goto M, Tamai N.. Membrane States of Lipids in Biological Membranes ― Structure-Function Relationship Revealed from Pressure Study. Review of High Pressure Science Technology. 2013;23:30-38.
[6] Mingotaud AF, Mingotaud C, Patterson LK. *Handbook of monolayers*. Vol. 1&2, ACADEMIC PRESS, San Diego. 1993.
[7] Mabrey S, Sturtevant JM. Investigation of Phase Transitions of Lipids and Lipid Mixtures by High Sensitivity Differential Scanning Calorimetry. *Proceedings of the National Academy of Sciences of the United States of America*. 1976;73:3862-3866.
[8] Luna EJ, McConnell HM. Multiple Phase Equilibria in Binary Mixtures of Phospholipids. *Biochimica et Biophysica Acta*,

1978;509:462-473.
[9] Caffrey M, Hing FS. A Temperature Gradient Method for Lipid Phase Diagram Construction Using Time-Resolved X-Ray Diffraction. *Biophysics Journal*. 1987;51:37-46.
[10] Poghosyan AH, Gharabekyan HH. Molecular Dynamics Simulation of DMPC/DPPC Mixed Bilayers, International Journal of Modern Physics C. 2007;18:73-89.
[11] González-Henríquez CM, Villegas-Opazo VA, Sagredo-Oyarce DH, Sarabia-Vallejos MA, Terraza CA. Thermal Response Analysis of Phospholipid Bilayers Using Ellipsometric Techniques. *Biosensors.* 2017;7:34.1-17.
[12] Rufeil-Fiori E, Wilke N, Banchioa AJ. Dipolar interactions between domains in lipid monolayers at the air-water interface. *Soft Matter*.2016;12:4769-4776.
[13] Arnold A, Cloutier I, Ritcey AM, Auger M. Temperature and pressure dependent growth and morphology of DMPC/DSPC domains studied by Brewster angle microscopy. *Chemistry and Physics of Lipids.* 2005;133:165-179.
[14] Matsuo H, Motomura K, Matsuura R. Mixed Monolayers of Dipalmitoylglycerophophocholine, Distearoylglycerophosphocholine and 1- Palmitoylglycerol. *Chemistry and Physics of Lipids.*1982;31:53-60.
[15] Lawrie GA, Gentle IR, Barnes GT. The structure of mixed monolayer films of DPPC and hexadecanol. *Colloids and Surfaces A: Physicochemical and Engineering Aspects*, 2000;171:217-224.
[16] Yoshida D, Yokoyama T, Shimoaki T, Tomita T, Yoshida T, Yamamoto Y, Taga K, Sumino A, Dewa T, Nango M, Yamamoto M, Sheravani Z. Morphology observation of dipalmitoyl phosphatidyl choline (DPPC) monolayer on water surface by dropping method. *Journal of Biophysical Chemistry.* 2013;4:115-121.
[17] Yamamoto Y, Taga K.. Lipid Monolayer and Interaction with Anesthetics. *Encyclopedia of Biocolloid and Biointerface Science.* 2016;1:36-58.
[18] Yokoyama T, Yoshida D, Mori H, Okabe M, Shervani Z, Taga K, Yamamoto Y, Sumino A, Dewa T, Nango M, Yamamoto M. Morphological Observation of Specific Condensation Effect of Cholesterol on Dipalmitoyl Phosphatidyl Choline (DPPC) Monolayer by Dropping Method. *Journal of Biophysical Chemistry*. 2016;7:98-109.
[19] Kobayashi Y, Amano T, Taga K, Yamamoto Y, Shervani Z, Yamamoto M. Surface Properties of Novel Surfactant, Dihexadecyl Gemini Phosphate, Monolayers on Water Surface by Dropping Method. *Journal of Biophysical Chemistry*. 2017;8:39-50.
[20] Okabe M, Taga K, Yoshino A, Yamamoto Y, Taneda A, Shinoda S, Kanamasa S, Shervani Z.. Effect of Escherichia coli on phospholipid monolayers: surface tensiometry and Brewster angle microscopy measurements. *European Biophysics Journal*. 2020;49:71-84.
[21] Yamamoto M, Suzuki M, Kimura T, Itoh K. Molecular structures at free surfaces of liquid n-heptadecane investigated by infrared external reflection spectroscopy. *The Journal of Physical Chemistry C*. 2008;112:13232-13239.
[22] Ohe C, Sasaki T, Noi M, Goto Y, Itoh K. Sum Frequency Generation Spectroscopic Study of the Condensation Effect of Cholesterol on a Lipid Monolayer. *Analytical and Bioanalytical Chemistry*. 2007;388:73-79.
[23] Yamamoto Y, Yokoyama T, Yoshida D, Mori H, Sekiguchi K, Shimoaki T, Yoshio A, Taga K, Shervani Z, Yamamoto M. Interactions between Phospholipid Monolayers (DPPC and DMPC) and Anesthetic Isoflurane Observed by Quartz Crystal Oscillator. *Journal of Biophysical Chemistry*. 2015;6:42-53.
[24] Ito D, Ikeda T, Taga K, Yamamoto Y, Shervani Z, Yamamoto M. Structural Change of Two Alkyl Chains in DMPC Molecule on DMPC- Cholesterol Mixed Monolayer -Specific Addition Effect of Cholesterol-. *Journal of Biophysical Chemistry*. 2019;10:15-29.
[25] Nakagaki M, Tomita K, Handa T. Interaction of Differently Oriented Lipids in Monolayer: Mixed Monolayers of 16-(9-Anthroyloxy) palmitic Acid with Phosphatidylcholine and Cholesterol. *Biochemistry*.1985;24:4619-4624.
[26] Janout V, Turkyilmaz S, Wang M, Wang Y, Manaka Y, Regen SL.. An Upside Down View of Cholesterol's Condensing Effect: Does Surface Occupancy Play a Role ?. *Langmuir*. 2010;26:5316-5318.
[27] Burn A, Brezesinsuki G, Möhwald H, Blanzat M, Perez E, Rico-Lattes I. Interaction between phospholipids and new Gemini catanionic surfactants having anti-HIV activity. *Colloids and Surfaces A: Physicochemical and Engineering Aspects*.2003;228:3-16.
[28] Yassine W, Milochau A, Buchoux S, Lang J, Desbat B, Oda R. Effect of monolayer lipid charges on the structure and orientation of protein VAMP1 at the air-water interface. *Biochimica et Biophysica Acta*, 2010;1798:928-937.
[29] Gaines GL. Insoluble monolayers at liquid-gas interface. Interscience Publishers, New York. 1966.
[30] Broniatowski M, Flasinski M, Dynarowicz-Latka P, Majewski J. Grazing Incidence Diffraction and X-ray Reflectivity Studies of the Interactions of Inorganic Mercury Salts with Membrane Lipids in Langmuir Monolayers at the Air/Water Interface. *Journal of Physical Chemistry B*. 2010;114:9474-9484.
[31] Miyoshi T, Kato S. Detailed Analysis of the Surface Area and Elasticity in the Saturated 1,2-Diacylphosphatidylcholine/Cholesterol Binary Monolayer System. *Langmuir.* 2015;31:9086−9096.
[32] Patterson M, Vogel HJ, Prenner EJ. Biophysical characterization of monofilm model systems composed of selected tear film phospholipids. *Biochimica et Biophysica Acta*. 2016;1858:403-414.
[33] Sabatini K, Mattila JP, Kinnunen PKJ. Interfacial Behavior of Cholesterol, Ergosterol, and Lanosterol in Mixtures with DPPC and DMPC. *Biophysical Journal.* 2008;95:2340-2355.
[34] Chapman D, Owens NF, Phillip MC, Walker DA. Mixed Monolayers of Phospholipids and Cholesterol. *Biochimica et Biophysica Acta*. 1969;183:458-465.
[35] Worthman LAD, Nag K, Davis PJ, Keough KM. Cholesterol in Condensed and Fluid Phosphatidylcholine Monolayers Studied by Epifluorescence Microscopy. *Biophysical Journal*. 1997;72:2569-2580.
[36] Kajiyama T, Tanimoto Y, Uchida M, Oishi Y, Takei R. Electro Microscopic Studies of Crystalline and Amorphous Monolayers of Fatty Acids. *Chemistry Letters*, 1989;2:189-192.
[37] Snyder RG, Strauss HL. C-H Stretching Modes and the Structure of n-Alkyl Chains. 1. Long, Disordered Chains. *Journal of Physical Chemistry*.1982;86:5145-5150.
[38] Knauf K, Meister A, Kerth A, Blume A. Interaction of alkyltrimethylammonium bromides with DMPC-d54 and DMPG-d54 monolayers studied by infrared reflection absorption spectroscopy (IRRAS), *Journal of Colloid and Interface Science*, 2010;342:243–252.
[39] Grossutti M, Seenath R, Lipkowski JInfrared and Fluorescence Spectroscopic Investigations of the Acyl Surface Modification of Hydrogel Beads for the Deposition of a Phospholipid Coating. *Langmuir.*2015;31:11598−11604.
[40] Yamamoto M, Sakurai Y, Hosoi Y, Ishii H, Kajikawa K, Ouchi Y, Seki K. Structures of a Long-Chain n-Alkane, n-C44H90, on a Au(111) Surface: An Infrared Reflection Absorption Spectroscopic Study, *Journal of Physical Chemistry B.* 2000;104:7363–7369.